SAND20XX-XXXXR

LDRD PROJECT NUMBER: 204724

LDRD PROJECT TITLE: Renewable hydrogen production via thermochemical/electrochemical coupling

PROJECT TEAM MEMBERS: Andrea Ambrosini (8824), Sean M. Babiniec (1514), James E. Miller (retired)

ABSTRACT:

A coupled electrochemical/thermochemical cycle was investigated to produce hydrogen from renewable resources. Like a conventional thermochemical cycle, this cycle leverages chemical energy stored in a thermochemical working material that is reduced thermally by solar energy. However, in this concept, the stored chemical energy only needs to be partially, but not fully, capable of splitting steam to produce hydrogen. To complete the process, a proton-conducting membrane is driven to separate hydrogen as it is produced, thus shifting the thermodynamics toward further hydrogen production. This novel coupled-cycle concept provides several benefits. First, the required oxidation enthalpy of the reversible thermochemical material is reduced, enabling the process to occur at lower temperatures. Second, removing the requirement for spontaneous steam-splitting widens the scope of materials compositions, allowing for less expensive/more abundant elements to be used. Lastly, thermodynamics calculations suggest that this concept can potentially reach higher efficiencies than photovoltaic-to-electrolysis hydrogen production methods. This Exploratory Express LDRD involved assessing the practical feasibility of the proposed coupled cycle. A test stand was designed and constructed and proton-conducting membranes were synthesized. While the full proof of concept was not achieved, the individual components of the experiment were validated and new capabilities that can be leveraged by a variety of programs were developed.

INTRODUCTION

Thermochemical cycles operate on the concept of converting thermal energy into chemical energy to drive subsequent chemical reactions. In brief, these cycles operate in two steps (Figure 1). In the first step, a “working” metal oxide material is heated above a temperature at which oxygen evolves from the structure. This leaves the material in a reduced state, where the thermal energy was converted to chemical energy represented by the material’s affinity to regain oxygen into its structure. In a second, lower-temperature step, the material is exposed to steam, where the oxygen in steam has a higher affinity to bond into the reduced metal oxide than it does to remain bonded with hydrogen atoms, which oxidizes the metal oxide and yields H_2. The names “oxygen carrier” and "redox material" are attributed to the ability for the material to lose and gain oxygen as well as transport chemical energy in the reduced state or oxygen in the oxidized state.

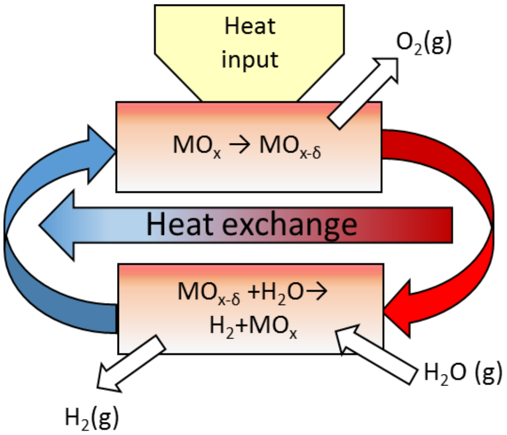

Figure 1: Illustration of a two-step thermochemical cycle.

Various metal oxide systems have been investigated as working materials for thermochemical cycles. These range from simple metal oxide pairs (ferrites, cobalt, Zn/ZnO), to blended oxides (cobalt ferrites), to mixed-ionic/electronic conducing (MIEC) oxides (ceria), to engineering perovskite MIECs[1,2,3,4]. One of the most successful steam-splitting redox materials is ceria due to its outstanding reaction kinetics and adequate thermodynamics to spontaneously split steam[3]. As these materials are reversible, the more affinity the material has for oxygen (increasing ability to split steam), the more difficult it is to remove the oxygen to reduce the material. This thermodynamic quantity is known as the reduction enthalpy. In the case of ceria, a reduction temperature of 1725 °C in air is required to achieve modest reduction of CeO_2 to $CeO_{1.95}$[5,6]. These extremely high temperatures and small reduction capacities result in limited choices for reactor construction materials, incompatibilities between the working material and reactor, limited choice of solar platforms, and reduced efficiencies.

In order to avoid the issues with reduction at such high temperatures, it is our goal to promote steam splitting *without* the requirement of spontaneous steam-splitting thermodynamics. This allows for a wide range of working materials options that exhibit lower reduction temperatures as well as enables the option to engineer materials to make them less expensive (by choosing earth-abundant cations) and to tune their performance (through material doping). However, in order to fully realize hydrogen production, the deficit in thermodynamic potential between the working material and steam splitting must be accounted for by another process. Our work focuses on coupling a proton-conducing membrane (PCM) to the thermochemical cycle in which the additional thermodynamic potential is electrically applied to the membrane, which operates as an electrochemical cell. This concept is coined "Electrically Enhanced Thermochemical Hydrogen Production", or EETHP.

Thermodynamically, the two-step cycle can be written as:

$$\text{Reduction: } 1/\delta\, ABO_3 + \Delta H_{red} \leftrightarrow 1/\delta\, ABO_{(3-\delta)} + 1/2\, O_2 \tag{1}$$

$$\text{Oxidation: } 1/\delta\, ABO_{(3-\delta)} + H_2O \leftrightarrow 1/\delta\, ABO_3 + H_2 \tag{2}$$

where δ is the oxygen non-stoichiometry in the material, otherwise known as the oxygen vacancy site concentration.

In either the direct thermochemical cycle or the EETHP cycle, Equation 1 remains the same, except that the quantity of ΔH_{red} differs, as EETHP does not require reduction so thermodynamically deep as to be able to spontaneously split steam. However, in the thermochemical cycle, the material is reduced deeply enough that the oxidation reaction occurs spontaneously, such that stoichiometric amounts of water and δ produce H_2. This is not the case in EETHP. Instead, small equilibrium concentrations of H_2 are produced, since the reduction enthalpy is not large enough to make the reaction is not spontaneous. However, the additional thermodynamic potential (ΔG) required to enable the reaction is provided by the electrochemical cell. Therefore, Equation 2 could be modified as such:

$$\text{Oxidation: } 1/\delta\, ABO_{(3-\delta)} + H_2O \ + \Delta G_{elect} \leftrightarrow 1/\delta\, ABO_3 + H_2 \qquad (3)$$

where ΔG_{elect} is the Gibb's free energy associated with the electricity provided to the electrochemical cell. This concept can be visualized in Figure 2. If the oxidation of the working material in steam is not spontaneous, there will be a very small equilibrium amount of hydrogen produced and then hydrogen production will stop once equilibrium is reached (Figure 2a). However, if the PCM is coupled, the hydrogen produced is continuously removed, preventing equilibrium concentrations from being reached, and hydrogen production is forced to continue (Figure 2b). This is commonly referred to as Le Chatelier's principle: reducing the concentration of products from a reaction shifts the reaction toward more products.

A full thermodynamic analysis was conducted to investigate the feasibility of the EEHTP concept[7]. This study assumed $SrMnO_{3-\delta}$ as the working material, primarily because it has a reduction enthalpy too low to split steam and the complete thermodynamic data for the material is published in the literature[8]. Not only did this study prove thermodynamic feasibility, but it also suggested high efficiencies of up to 25% for renewable hydrogen production.

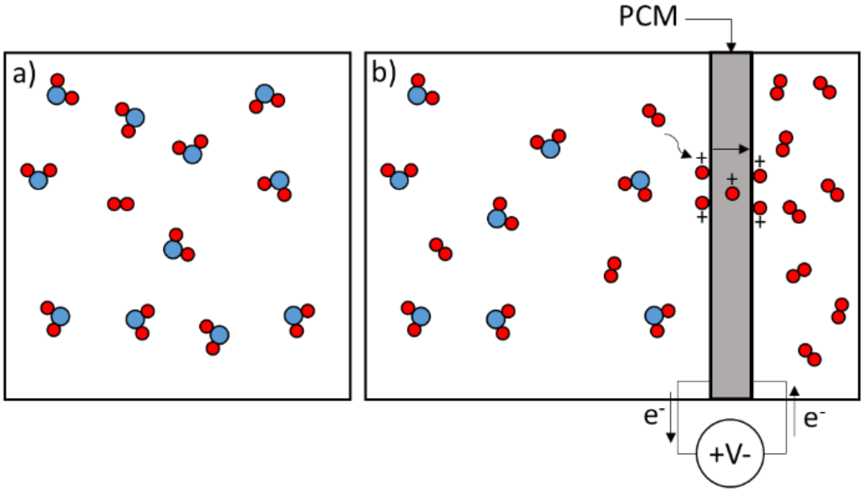

Figure 2: Illustration of non-spontaneous oxidation in steam a) without coupled PCM, and b) with coupled PCM.

Our primary technical objective is to conduct a lab-scale proof of concept demonstration of the proposed idea with the following outcomes 1) demonstrate the validity of the chemical approach, and 2) provide validation of our thermodynamic calculations indicating the concept can be applied to split water with high efficiency. A secondary outcome will be determining the applicability of PCMs to characterize the kinetics of steam oxidation of reduced oxides.

DETAILED DESCRIPTION OF EXPERIMENT/METHOD

In order to investigate coupled oxidation of the working material, several facets of experimentation had to be addressed. These include test stand construction, materials synthesis and cell fabrication, electrochemical testing, and gas analysis.

Materials synthesis: The proton-conduction membrane (PCM) synthesized for the test cell was $BaCe_{0.1}Zr_{0.8}Y_{0.1}O_{3-\delta}$ (BCZY18, a known proton conducting electrolyte[9,10]. The materials was synthesized using a Pechini solution method, wherein stoichiometric (metals basis) amounts metal nitrate/oxynitrate hydrate precursors were dissolved in H_2O with citric acid as a chelating agent. $Ni(NO_3)_2{\cdot}6H_2O$ was also added (corresponding to a 1 wt.% NiO concentration) as a sintering agent. The solution was heated with stirring until most of the H_2O evaporated and a viscous gel formed. The gel was dried overnight at 100 °C, resulting in a dried foam. The nitrates were burned off by heating the powder, resulting in a fine powder of intimately-mixed metal oxide. The powder was calcined for several hours at 800 °C to remove any remaining organics/nitrates and the resulting powder was sieved to obtain particles < 90 μm in size. The powders were mixed with 2-4 wt.% polyvinyl butyral binder and ground with an agate mortar and pestle. The resulting mixture was pressed into a 25 cm diameter pellet (approx. 1-2 mm thick) and sintered for 48 hours at 1375 °C. (This temperature is the upper limit of our in-house furnace.) When this temperature seemed insufficient, subsequent membranes were sintered an additional 24-48 hours at 1600 °C using a different furnace located at Sandia's Advanced Materials Lab.

$CaAl_{0.2}Mn_{0.8}O_{3-\delta}$ (CAM28) working material was also synthesized using a solution Pechini method. Stoichiometric amounts of nitrate salts were dissolved in water, then citric acid was added to the solution in a 1:1 molar cation:citric acid ratio. The solution was dried and combusted, and the resulting ash was pre-calcined at 850 °C for 2 hours in air. These powders were mixed with 1.5 wt.% polyvinyl butyral (PVB) and pressed in a ⌀ 13 mm die at 35 MPa. Pressed pellets were sintered at 1250 °C for 48 hours in air. The resulting product, which crystallizes in the orthorhombic perovskite structure (identified using X-ray powder diffraction), was then ground up into powder and sieved to the desired particle size for use in the electrochemical cell.

Test stand construction: The test stand was constructed using a ATS 3210 split-tube furnace mounted in a Unistrut cage. Custom alumina manifolds were machined by O'Keefe Ceramics to accommodate a 1" electrochemical cell and mate to ¾" alumina tubes (Figure 3). Gas delivery and electrical feedthroughs were fabricated using PTFE disks and were sealed via O-rings in the cold zone of the test stand. Hot zone seals within the alumina manifolds were accomplished using

Flexitallic Thermiculite 886 compression seals. Argon was delivered to the top and bottom sides of the cell through Agilent mass-flow controllers (MFCs) capable of 0-500 ml/min gas flow. The top gas stream was also switchable to 2.9% H_2/ Ar balance with the option to humidify the gas stream through a bubbler chamber filled with DI water. A manifold was designed at the output to send either the top or bottom side to gas analysis or venting, whichever is required by the particular test being conducted.

Electrochemical cell fabrication: To construct the electrochemical cell, the membrane was placed in the manifold with compressive seals on either side. Silver mesh (99.999%) was used as an electrode and silver paste (ESL, Inc) was used to attach four-point electrical contacts fabricated from silver, such that there is both a current collect/supply wire and a voltage probe wire on each side of the cell. 1-2 grams of CAM28 powder was placed into the particle bed chamber on reactive (H_2/Ar or steam) side of the cell. The membrane cell was assembled into the test cell, which was then plumbed with the necessary gases and place in a vertical tube furnace. (Figure 4)

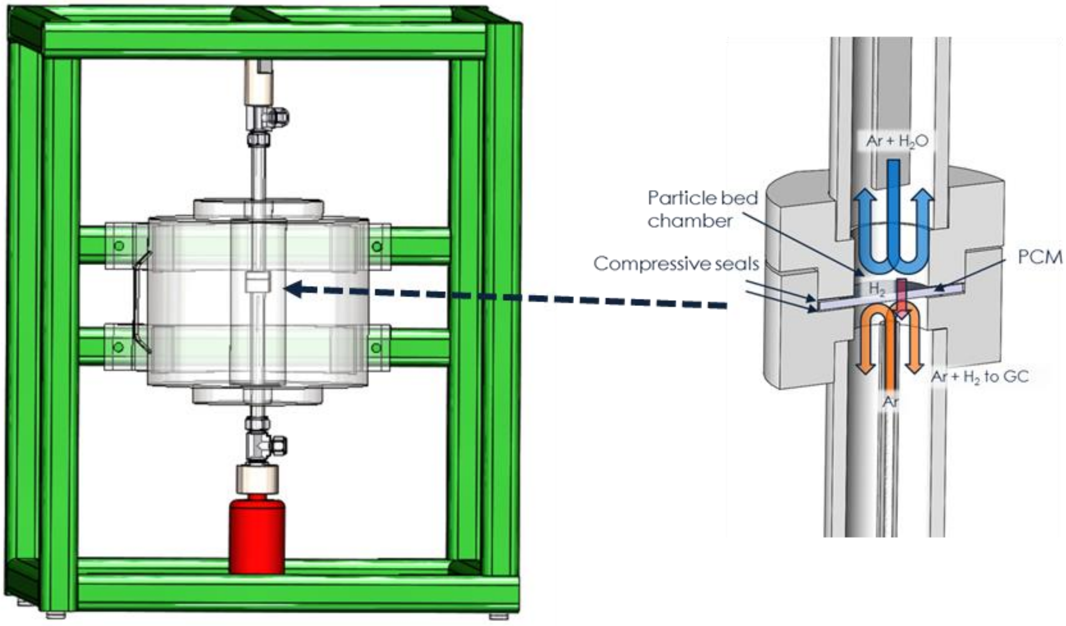

Figure 3: Design of compressively-sealed test stand (left) and detail of manifold design (right).

Electrochemical measurements and gas analysis: Electrochemical experiments were driven by a Solartron 1287 potentio/galvanostat. Open-circuit voltage was measured during cell heating and during gas environment changes. The cell was polarized in a galvanostatic fashion, where a constant current was applied in the direction of promoting hydrogen transport while the voltage was monitored. Concurrently, the gas composition was monitored with an Agilent G2082A micro gas chromatograph (μGC) utilizing a Molsieve column with Ar carrier gas to quantify evolution or consumption of gas species.

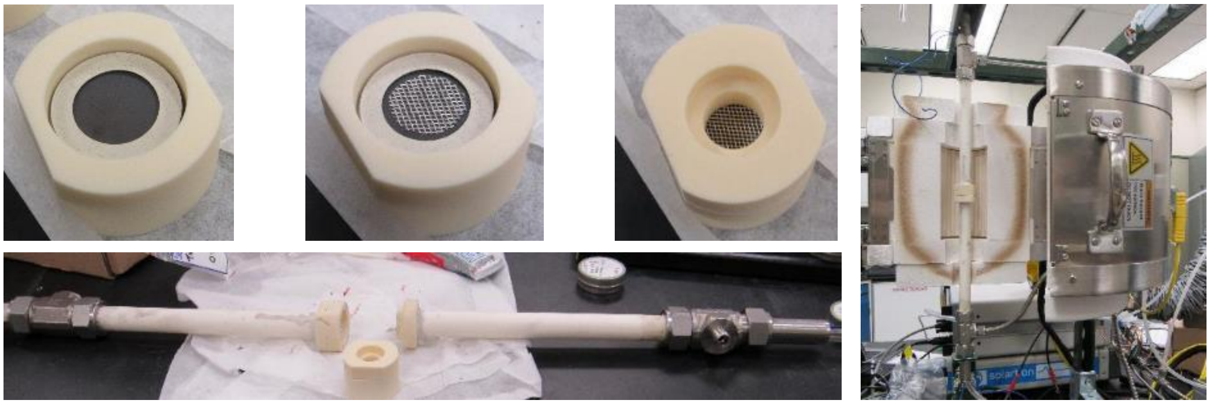

*Figure 4: **Top**: assembly of membrane cell. **Middle**: test cell. **Bottom**: assembled test cell plumbed and in furnace.*

RESULTS:

The thermo-electrochemical test stand was designed and constructed as described and illustrated above. The test cell was successfully heated to 650 °C, and the connections, plumbing, gas flow, electrode connections, and gas analyses were verified to operate at temperature.

Producing a non-porous (> 90% theoretical density) flat PCM of BCZY18 was more of a challenge than anticipated. The first attempts, which involved pressing the precursor powder after the initial calcine into 25 cm disks and sintering at 1375 °C, resulted in warped porous discs that were unusable in the test cell. New membranes were synthesized, and an extra sieving step was added after the addition of binder. The powder was sieved to achieve particle sizes ≤ 90 μm in order to assure more homogeneous particle size and achieve less warpage and higher density. After sintering at 1375 °C, the membranes had improved structural properties, i.e. less warpage, but were still porous. The membranes were sintered again at 1600 °C, resulting in slightly denser membranes, but were not completely gas impermeable. Dip-coating the sintered pellets in precursor nitrate solution followed by an additional 8-hour sinter at 1375 °C was attempted in order to fill the pores, but full density was still not achieved. In the interest of deadlines, however, experiments were conducted with the most promising-looking membranes.

The open circuit behavior of the cell was measured while flowing 2.9% H_2/Ar on the reactive side and an Ar sweep on the other. The agreement between the measured value versus the predicted behavior is shown in Figure 5. In addition, an open circuit voltage (OCV) was observed when the feed gas was switched from 2.9% H_2/Ar to steam/Ar. A small presence of H_2 was detected in the presence of steam via gas chromatography, indicating that the reduced thermochemical working material (CAM28) was at least partially active.

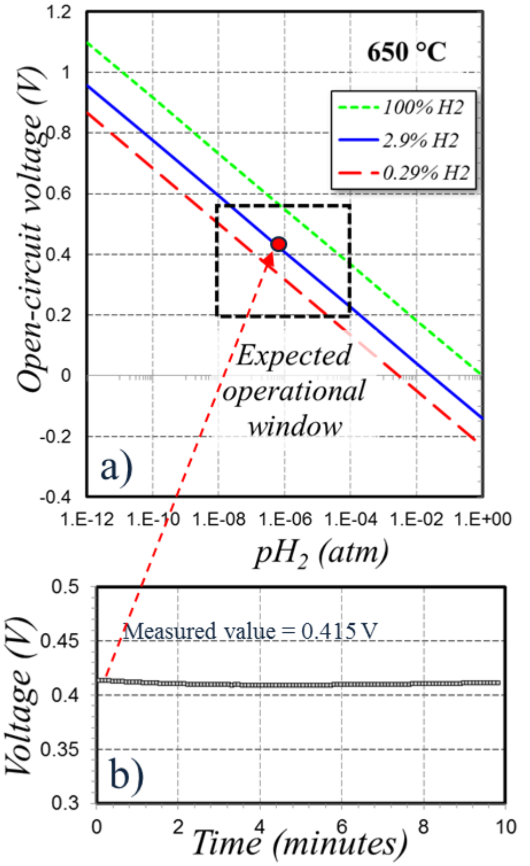

Figure 5: (a) OCV as a function of pH2 on sweep side. (b) Measured open-circuit voltage.

The next planned experiment over the course of the project was to verify that the proton conducting membrane (PCM) of BCZY18 was effectively transporting hydrogen. This was initially performed by exposing the reactive side of the cell to H_2/Ar and detecting the transported H_2 on the Ar sweep side of the cell. However, this planned experiment was thwarted by the presence of large O_2 and N_2 peaks on the μGC, indicating the presence of air, likely from a leak. Attempts to locate and ameliorate the leak were unsuccessful. No leak was observed on the active side of the cell. Therefore, an alternative experiment was designed and executed, which involved monitoring the concentration of H_2 on the H_2/Ar active side as a function of current. Theoretically, as the current to the membrane increases, so should the proton transport across the PCM. This should result in a decrease in H_2 concentration of the H_2/Ar gas on the active side of the electrochemical cell. Figure 6 shows the percentage of H_2 in the sweep gas, calculated from the decrease observed via μGC in the H_2 concentration in 2.9% H_2/Ar, versus current. While there is a slight increase in concentration, it does not reach the calculated Faradaic limit. However, the change in concentration does illustrate that some hydrogen transport is taking place.

In order to prove successful thermochemically-assisted hydrogen production as alluded to in our proposal, it must be shown that hydrogen is (1) produced from steam and (2) transported across the PCM. Due to the aforementioned leak on the sweep side of the cell, direct measurement of H_2 was not possible. Instead, a new experiment was developed in which the voltage at a given current was observed over a duration of several hours. The hypothesis behind this experiment was that if hydrogen production is thermochemically-assisted, the observed voltage should increase when the available thermochemical inventory is consumed, e.g. when the reduced working material is fully reoxidized by steam. The amount of the CAM28 working material was estimated to last for 3 hours of H_2 production assuming a Faradaic efficiency of 1.0; therefore, the experiment was set to run for 5 hours to ensure completion. Figure 7 shows the expected behavior versus the observed performance of the test cell. As evidenced, the expected increase in voltage was not observed after five hours.

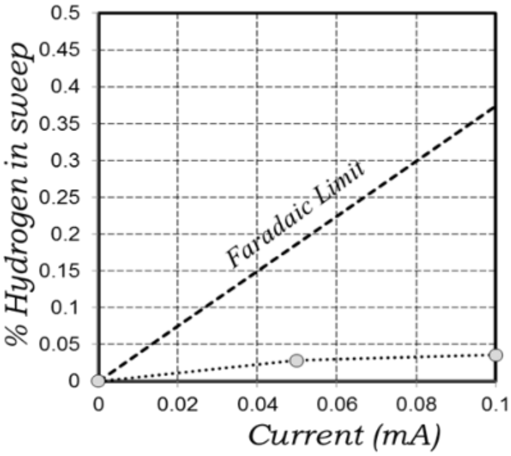

Figure 6: Hydrogen transport performance: 2.9% H_2/bal. Ar vs. Ar, 650 °C.

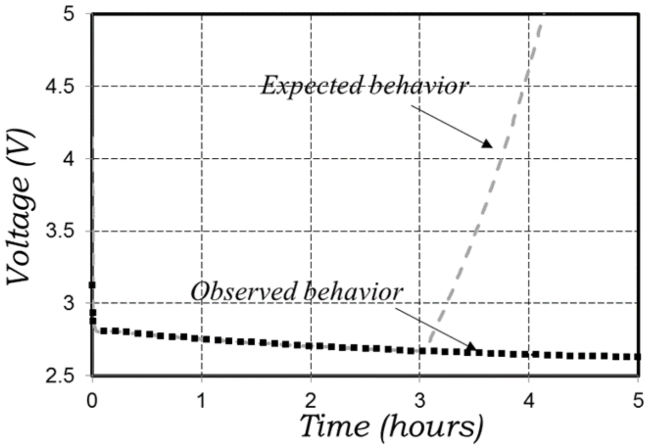

Figure 7: Expected vs. observed behavior of voltage over reaction time during assumed thermochemically-assisted H_2 production.

DISCUSSION:

Working materials: Both BCZY18 and CAM28 were chosen as the PCM and thermochemical working materials, respectively, due to the team's familiarity with the materials. BCZY18 has a proven track record as a proton conductor [9,10]. CAM28 has been extensively studied and characterized as a redox-active material for concentrating solar power thermochemical heat storage[11]. The thermodynamic properties of CAM28 are known and it theoretically should split water under the thermo- and electro-chemical conditions present in the test cell.

While the CAM28 powder was successfully obtained, challenges were encountered in synthesizing a fully-dense, flat membranes of BCZY18. Powder x-ray diffraction confirms that the expected perovskite phase was obtained. As described in the Results section, sieving the particles to reduce size distribution and pressing thicker membranes proved helpful in limiting the warpage, but were not sufficient to fully densify the membrane. One possible cause may be the sintering temperature. In previous preparations, BCZY compositions were coated onto supports and sintered at 1600 °C. The presence of a support like inhibited any warpage. In our case, the material was made as a stand-alone membrane and originally sintered to 1375 °C, due to temperature limits in the available furnace. It was anticipated that the intimate mixing and small particle size of the precursor powders that are obtained as a result of the Pechini solution prep (vs. solid state methods) would compensate for the lower sintering temperature. However, that seems to not be the case. Post-sintering at 1600 °C did not solve the issue either; it's possible that the second sintering step was ineffective due the loss of binder and NiO sintering aid during the first step. In other words, the microstructure that formed at 1375 °C could not be overcome by additional heating. Because of the impending project deadlines, however, it was decided to move forward with most promising membranes amongst the synthesized cohort. In future experiments, the pressed membrane will be sintered directly at 1600 °C in order to potentially overcome this issue.

Electrochemical cell performance: The open circuit behavior of the cell was calculated as a function of partial pressure of H_2 on the sweep side of the call at 650 °C (Figure 5a) for several concentrations of H_2 on the active side. The area of interest for this set of experiments are found in the boxed area. The observed OCV under the experimental conditions of 2.9% H_2/Ar fits well with the calculated values (Figure 5b), indicating that the membrane is electrochemically active, despite the presence of porosity. An OCV was also observed when the feed gas was switched to steam/Ar. In addition, a small amount of H_2 was detected via μGC on the active side, implying that the CAM28 working material is also active.

The proton conducting properties of the BCZY18 membrane were investigated electrochemically as well, by measuring the flux of protons through the PCM as a function of current. Since the aforementioned leak prevented the direct measurement of H_2 evolution on the sweep side, the H_2 concentration on the active side of the cell was measured, under the assumption that transport of protons across the PCM to the sweep side will result in a decrease of H_2 on the active side. Figure 6 shows the results. A slight increase in current was measured, indicating some proton transport, but it does not come close to the calculated Faradaic efficiency of the cell membrane. The observed low Faradaic efficiency can be attributed to several possible causes, related to cell assembly. These include a poor membrane seal, either due to slight warpage or faulty O-ring. This may also be the source of the leak detected on the sweep side of the test cell. The porosity of the membrane may also play a role in the poor performance. Finally, there may be electronic leakage in the membrane as a result of additional charge carriers (electrons, holes, and/or oxides) which may form as a function of gas environment and voltage. While normal operating conditions should not favor additional carrier formation, the presence of air due to a leak of some sort may result in their creation.

Hydrogen production: The ultimate proof of concept of the theorized coupled thermochemical/electrochemical production of hydrogen is to show that hydrogen is (1) produced from steam and (2) transported across the PCM. As described in the Results section, the existence of a leak on the sweep side of the cell prevented direct monitoring of hydrogen production via steam-splitting and subsequent transport across a proton conducting membrane. The alternate experiment to measure steam splitting activity via observing voltage over time (Figure 7), with the expectation that the voltage would jump after the CAM28 fully reacted, also did not yield expected results. There can be several reasons for this. (1) Low faradaic efficiency resulted in less hydrogen transported, thus thermochemical material not oxidized by end of experiment. I.e., the water splitting reaction was not driven to completion due to lackluster proton transport through the PCM. (2) The thermochemical material did not adequately reduce at 650 °C under 2.9% H_2/Ar. Although thermodynamic calculations can accurately predict the extent of reduction of CAM28 at a given temperature and atmosphere, the unintended exposure to air, e.g. from a leak, could cause unintended oxidation. (3) Kinetic limitations hindered thermochemical assistance. In other words, reoxidation of the working material by steam proceeded too slowly to be effective.

CONCLUSION:

The milestone of this EE LDRD was to achieve the lab-scale demonstration that couples thermal/electrochemical hydrogen production that provides a renewable thermal route to hydrogen from water at system thermal efficiency of > 20% (including thermal equivalent of electrical demand) and a peak system temperature of < 1200 ºC. While the project fell somewhat short of this goal in the time allotted, several important things were achieved. A novel test stand to prove the concept was conceptualized and constructed. The test cell was successfully heated to 650 °C without incident. Proton transport across the BCZY18 membrane was demonstrated, as was the water splitting activity of the CAM28 working material. In short, the individual components of the experiment were validated, but assembly issues hindered the demonstration of the integrated system. The two main issues hindering success are the quality of the membrane and poor sealing in the test stand. However, we believe that these challenges are mechanical in nature and can be mitigated relatively easily. In other words, the main barriers to demonstration of this concept are engineering issues, not scientific ones. We remain confident in the soundness of our theory and our ability to demonstrate a working system.

ANTICIPATED OUTCOMES AND IMPACTS

Next steps: Immediate steps that we would take going forward in order to meet our Milestone include the following:

- Use lessons-learned to fabricate improved membranes, with minimum porosity and warpage
    - Sinter directly to 1600 °C without intermediate 1375 °C step
    - Determine best precursor particle size and distribution to prevent warpage and maximize density
- Solve sealing issues
    - Top manifold seal functioned properly but must investigate why bottom seal was compromised
    - Leak-test entire system before heating test cell
- Once seal and membrane issues are resolved, repeat intended experimental set but this time obtain direct (versus implied) results by detecting and quantifying H_2 in Ar sweep gas. Verify:
    - Thermochemical activity of CAM28 working material
    - Proton transport through BCZY18 PCM
    - Thermochemically-assisted electrolysis is more efficient than electrolysis alone
- Analyze steam/H_2O concentrations in reaction cell for full characterization of gas streams
    - Current μGC configuration (Molsieve column) does not detect H_2O

  - Mass spectrometry could be utilized to fully characterize gas compositions

Future steps: After demonstrating proof of concept, we would propose these activities as part of any future funded projects.

- Fully characterize system by varying applied current, reduction extent of working material, reaction temperature
  - Quantify transport efficiency and kinetic limitations of PCM
  - Extract thermodynamic information: with denser membranes, OCV with and without thermochemical material could provide analysis of the change in thermodynamic state due to the presence of thermochemical material
- Materials development
  - Decreased reaction temperatures greatly broaden the field of promising redox-active materials compositions for thermochemical steam splitting
  - Leverage current materials development efforts underway for Sunshot-funded CSP thermochemical energy storage (PROMOTES), e.g., CAM28
  - Investigate new materials compositions for proton conducting membranes
- Utilize the capabilities at the National Solar Thermal Test Facility (solar simulator, solar furnace) at Sandia to couple reactor to a concentrating solar power source to determine feasibility of developing a fully renewable process

Resulting publications/patents:

- Provisional patent: Patent No. 62/461,141 filed on 2 February, 2017
  - We will utilize current and future results to move this provisional patent to full patent
- Publications
  - S.M. Babiniec, A. Ambrosini, J.E. Miller, "Thermodynamic assessment of an electrically-enhanced thermochemical hydrogen production (EETHP) concept for renewable hydrogen generation", *Int. J. Hydrogen Energy* 42, 14380-14389, 2017.
  - Follow-on paper planned after more data is accumulated

Impact:

- The test stand is a new capability can be leveraged for testing a variety of application relevant to Sandia programs, such as solid oxide fuel cell/electrolyzer materials, thermochemical H_2 and fuels production, thermodynamic measurements of redox active materials
- Mission relevance: Directly addresses SNL's SSEF mission space and DOE and EERE mission areas, e.g. DOE's HydroGEN Advanced Water Splitting Materials (Sandia is a core laboratory)
- Successful demonstration of this process can enable increased efficiency of H_2 production utilizing renewable resources (CSP, PV, H_2O), which will enhance and secure America's energy future

- Increased visibility of Sandia R&D via publications and presentations at national conferences

Upcoming funding opportunities and partners:

Potential partners going forward include both internal Sandia departments including 8823 (NSTTF), 8367 (Hydrogen and Materials Science), and 1815 (AML), as well as external collaborators such as Colorado School of Mines (thermochemical energy storage, PCM development), Arizona State University (technoeconomic and systems analyses), and Georgia Institute of Technology (Academic Alliance, solar fuels and technologies).

Sandia is a core laboratory for DOE's HydroGEN Advanced Water Splitting Materials effort. The team will endeavor to find support within this energy materials network (EMN) both directly (i.e., internally) and as a resource to external partners. The team also intends to apply for an LDRD to perform necessary follow-on R&D, such as materials discovery and optimization, both computationally and conventionally, for both PCMs and active metal oxides, kinetic and thermodynamic characterization, and integration with renewable power sources. The team will also apply to external FOAs as applicable; potential funding sources include ARPA-E, SunShot, and Fuel Cells and Technology Office.

---

1 Roeb M, Neises M, Monnerie N, Call F, Simon H, Sattler C, et al. Materials-related aspects of thermochemical water and carbon dioxide splitting: a review. Materials 2012;5:2015-54. http://dx.doi.org/10.3390/ma5112015.

2 Agrafiotis C, Roeb M, Sattler C. A review on solar thermal syngas production via redox pair-based water/carbon dioxide splitting thermochemical cycles. Renew Sustain Energy Rev 2015;42:254-85. http://dx.doi.org/10.1016/j.rser.2014.09.039.

3 Miller JE, McDaniel AH, Allendorf MD. Considerations in the design of materials for solar-driven fuel production using metal-oxide thermochemical cycles. Adv Energy Mater 2014;4:1300469. http://dx.doi.org/10.1002/aenm.201300469.

4 Scheffe JR, Steinfeld A. Oxygen exchange materials for solar thermochemical splitting of H2O and CO2: a review. Mater Today 2014;17:341e8. http://dx.doi.org/10.1016/j.mattod.2014.04.025.

[5] Zinkevich M, Djurovic D, Aldinger F. Thermodynamic modelling of the cerium-oxygen system. Solid State Ionics 2006;177:989-1001. http://dx.doi.org/10.1016/j.ssi.2006.02.044.

[6] Palumbo R, Larson C, Guertin J, Schoer J, Meyer M, Diver RB, et al. Solar thermal decoupled water electrolysis process I: proof of concept. Chem Eng Sci 2012;84:372-80. http://dx.doi.org/10.1016/j.ces.2012.08.023.

[7] Babiniec SM, Ambrosini A, Miller, JE. Thermodynamic assessment of an electrically-enhanced thermochemical hydrogen production (EETHP) concept for renewable hydrogen generation. Int. J. Hydrogen Energy 2017;42;14380-14389.

8 Rørmark L, Mørch AB, Wiik K, Stølen S, Grande T. Enthalpies of oxidation of $CaMnO_{3-\delta}$, $Ca_2MnO_{4-\delta}$, and $SrMnO_{3-\delta}$ - deduced redox properties. Chem Mater 2001;13:4005-13.

---

[9] Babiniec SM, Ricote S, Sullivan NP. Characterization of ionic transport thought $BaCe_{0.2}Zr_{0.7}Y_{0.1}O_{3-\delta}$ membranes in galvanic and electrolytic operation. Int. J. Hydrogen Energy 2015; 30; 9278-9286.

[10] Dippon M, Babiniec SM, Ding H, Ricote S, Sullivan NP. Exploring electronic conduction through $BaCe_xZr_{0.9-x}Y_{0.1}O_{3-\delta}$ proton-conducting ceramics. Solid State Ionics 2016; 286; 117-121.

[11] Babiniec SM, Coker EN, Miller JE, Ambrosini A. Doped calcium manganites for advanced high-temperature thermochemical energy storage. Int. J. Energy Research 2016; 40; 280-284.

Sandia National Laboratories is a multimission laboratory managed and operated by National Technology and Engineering Solutions of Sandia LLC, a wholly owned subsidiary of Honeywell International Inc. for the U.S. Department of Energy's National Nuclear Security Administration under contract DE-NA0003525.